Reports

Solar-Type Xenon: A New Isotopic Composition of Xenon in the Pesyanoe Meteorite

Abstract. *Xenon in the Pesyanoe meteorite is a mixture of several components. Solar-type xenon is a new component deficient in the neutron-rich isotopes as compared to both trapped chondritic and terrestrial atmospheric xenon.*

Since the first report of a new isotopic composition of xenon in the Pesyanoe enstatite achondrite (*1*), additional data have been obtained (*2*). There can be little doubt that the new isotopic composition of xenon in the Pesyanoe meteorite is due to the presence of a solar-type gas component. A report at the present time is desirable for the following reasons. (i) Solar wind gases, including probably Xe, are present in samples from the lunar surface. It will be of great interest to compare the solar wind composition on the lunar surface with solar-type gases in the Pesyanoe meteorite. (ii) The fact that the neutron-rich isotopes of xenon have lower relative abundances in the Pesyanoe meteorite than in either chondritic meteorites or atmospheric xenon is important for future work on fission-type xenon.

The results of the analysis of two samples of the Pesyanoe enstatite achondrite are given in Table 1. The gases of sample I (0.94 g) were extracted in a one-step melting procedure. Sample II (0.66 g), which contained less of the grayish fine-grained material, was heated stepwise, and the released gases were recovered in three fractions at different temperatures. The isotopic abundances of trapped chondritic xenon (*3*) and of atmospheric Xe (*4*) are given in Table 1 for comparison. Inspection of the results for both samples and temperature fractions indicates an isotopic composition generally similar to that of trapped chondritic xenon but with (i) clear excesses of Xe^{126} and Xe^{124} and smaller excesses of Xe^{128} and Xe^{130}, and (ii) clear deficiencies of the heavy isotopes Xe^{134} and Xe^{136}. All the excesses of the neutron-poor isotopes can be attributed to cosmic-ray spallation based on the following arguments: (i) the mass yield spectrum of the excesses is similar to known spallation spectra (*5*); (ii) a subtraction of xenon in the two samples (sample I minus sample II) lowers the relative abundances of the light isotopes, leaving the others unchanged; and (iii) from the excess Xe^{126} and a cosmic-ray age of 43 million years (*6*), Xe^{126} production rates of 0.0022×10^{-12} cm^3 (at standard temperature and pressure) per gram per million years (sample I) and 0.0018×10^{-12} cm^3 (at standard temperature and pressure) per gram per million years (sample II) are obtained; these values are lower by about a factor of 3 than chondritic production rates but intermediate to those calculated for the Norton County and Khor Temiki meteorites, two other enstatite achondrites (*7*). A correction for cosmic-ray spallation does not affect the abundances of the neutron-rich isotopes Xe^{134} and Xe^{136}. The only possible correction for *in situ* nuclear processes, a correction for fission products, would further lower the relative abundances of the heavy isotopes.

In Fig. 1 δ-values, defined as

$$\delta^{M}{}_{132}(\%) = 100\left[\frac{Xe^{M}/Xe^{132}\,(\text{meteorite})}{Xe^{M}/Xe^{132}\,(\text{atmosphere})} - 1\right]$$

are plotted for the total xenon in the Pesyanoe meteorite and for the fraction recovered at 1000°C, both of

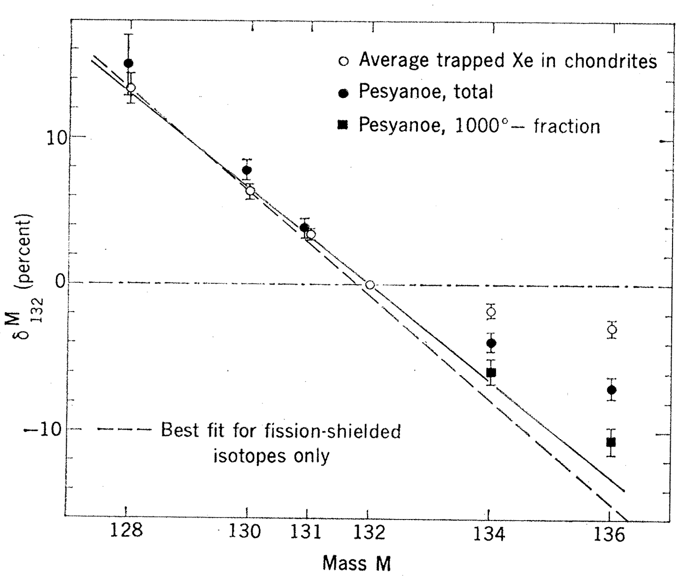

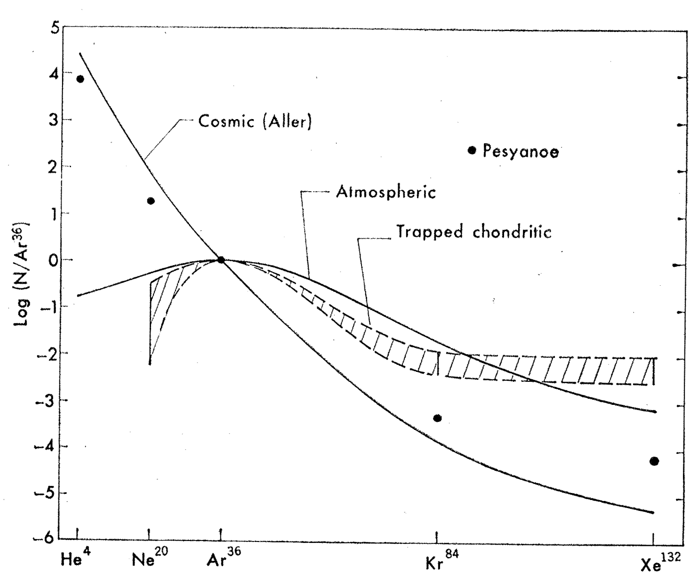

Fig. 1 (left). Values of $\delta^{M}{}_{132}$ for Xe^{128} to Xe^{136} in the total and 1000° fraction of the Pesyanoe meteorite are compared to those of average trapped Xe in chondrites. The solid line is a best fit to the isotopes Xe^{124} to Xe^{132} of average trapped chondritic Xe, whereas the dashed line is a fit to the fission-shielded isotopes Xe^{124} to Xe^{130} only; Xe^{129} is excluded. Fig. 2 (right). Relative rare-gas abundances normalized to Ar^{36} in the Pesyanoe meteorite and in chondrites are compared to terrestrial atmospheric and cosmic abundances (see Table 2).

Table 1. Isotopic composition and contents of xenon [$\times 10^{-12}$ cm^3 (at standard temperature and pressure) per gram] in two samples of the Pesyanoe meteorite. The isotopic abundances are normalized to Xe^{132} = 100 percent.

Xenon	Xe^{132}	Isotopic composition (percent)								
		Xe^{124}	Xe^{126}	Xe^{128}	Xe^{129}	Xe^{130}	Xe^{131}	Xe^{132}	Xe^{134}	Xe^{136}
Sample I	96 ± 12	0.488 ± 0.015	0.504 ± 0.012	8.28 ± 0.10	103.3 ± 0.8	16.40 ± 0.11	82.0 ± 0.4	100	37.3 ± 0.3	30.7 ± 0.3
Sample II										
700° fraction	10.7	0.44 ± 0.02	0.45 ± 0.03	7.80 ± 0.15	101.6 ± 1.0	15.9 ± 0.2	79.4 ± 0.5	100	38.4 ± 0.4	31.9 ± 0.4
1000° fraction	24.1	0.49 ± 0.02	0.53 ± 0.02	8.30 ± 0.15	104.1 ± 0.9	16.5 ± 0.2	81.7 ± 0.5	100	36.5 ± 0.3	29.5 ± 0.3
1600° fraction	29.2	0.52 ± 0.02	0.55 ± 0.02	8.14 ± 0.12	103.7 ± 0.8	16.3 ± 0.2	82.4 ± 0.6	100	37.7 ± 0.4	31.0 ± 0.3
Total	64.0 ± 7.7	0.495 ± 0.022	0.526 ± 0.022	8.14 ± 0.14	103.5 ± 0.9	16.3 ± 0.2	81.6 ± 0.5	100	37.4 ± 0.35	30.6 ± 0.35
Trapped Xe (*3*)		0.452	0.406	8.09	(102.4)	16.13	81.5	100	38.1	32.0
Atmospheric Xe (*4*)		0.357	0.335	7.14	98.3	15.17	78.8	100	38.8	33.0

which can be compared to values for trapped Xe in chondrites and for terrestrial atmosphere Xe (used for normalization); Xe^{124} and Xe^{126} are not shown here because of the large relative spallation excesses. The abundances of isotopes Xe^{128} to Xe^{131} of the 1000° fraction agree with those in the bulk samples within the limits of error and are not plotted. Corrections for spallation, as discussed above, shift the Pesyanoe points of masses 128 to 131 even closer to those of average chondritic Xe.

The discrepancies of the Xe^{134} and Xe^{136} points indicate that xenon in the Pesyanoe meteorite presents a new isotopic composition. While excesses in the heavy Xe isotopes due to fission xenon have recently been found in several meteorites, Pesyanoe is the first one with a clear-cut deficiency. The 1000° fraction has even lower relative abundances. The data from a stepwise heating of the Fayetteville meteorite, another gas-rich meteorite (*8*), also show a temperature fraction (800°C) with deficiencies of Xe^{134} and Xe^{136}. The importance of this fact has not been realized. Closer inspection of the Pesyanoe data reveals a perfect agreement of the two sample totals, but there are differences well outside the limits of error among the three temperature fractions. The δ-values given in Fig. 1 for the isotopes Xe^{132}, Xe^{134}, and Xe^{136} form nearly linear arrays of different slopes. This is also true for the two temperature fractions not shown in Fig. 1. Such a variation in the Xe released at different temperatures (variation in $\delta\,^{132}_{136}$ up to 7 percent) can be understood only for a system containing more than one component. In a mixture of two or more components, one component must have isotopic abundances of Xe^{134} and Xe^{136} equal to or lower than those of the 1000° fraction and must have the trapped chondritic composition for all other isotopes. This is a new Xe component which we call "solar-type" for the following reasons.

1) Figure 2 shows the relative elemental abundances for the rare gases He to Xe, normalized to Ar^{36}. The Pesyanoe pattern is typical for gas-rich meteorites and is different from either the atmospheric or the trapped chondritic composition (see Table 2). Signer and Suess (*9*) termed this component "solar," because of a close resemblance to the solar or cosmic abundance pattern.

2) The abundances of Kr and Xe, relative to Ar, in the Pesyanoe meteorite, are somewhat higher than estimates in compilations of cosmic abundance (Table 2). However, these cosmic abundances are not too well known; errors by a factor of 2 or 3 are entirely possible. The contents of Kr^{84} and Xe^{132}, as found here in the two samples, compare favorably with the values that Zähringer (*10*) has reported as upper limits. The measured abundance ratios Kr/Xe are much larger than those in other meteorites. Ratios of Kr^{84}/Xe^{132} greater than 4 are found in only a few gas-rich meteorites and therefore are diagnostic for the presence of solar-type gases. Therefore, some of the Xe and a sizable fraction of the Kr must belong to this component.

There is no indication of a deficiency of the heavy krypton isotopes. The relative abundances (sample I) are Kr^{78} : Kr^{80}: Kr^{82}: Kr^{83}: Kr^{84}: Kr^{86} = 2.03 ± 0.03: 13.23 ± 0.13: 65.8 ± 0.4: 66.1 ± 0.4: 324.7 ± 1.8: 100, and the Kr^{86} content is $205 \pm 25 \times 10^{-12}$ cm^3 (at standard temperature and pressure) per gram. Again, small excesses of Kr^{78} to Kr^{84} can be attributed to cosmic-ray spallation. After such a correction, an isotopic composition very similar to that of trapped chondritic krypton is obtained. Solar-type krypton therefore is not detectably different from trapped chondritic krypton. In Table 2 the relative abundances of He, Ne, Ar, Kr, and Xe in the Pesyanoe meteorite are compared to those in the terrestrial atmosphere, to those in chondrites, and to various estimates for cosmic abundances. Values labeled "Pesyanoe-A" represent the averages of the measured abundance ratios. In this case, it is assumed that all measured Kr^{84} and Xe^{132} belong to the solar-type component, and that the variation in the heavy xenon isotopes in the temperature fractions of the Pesyanoe meteorite is due to the presence of a hypothetical fission component. Values labeled "Pesyanoe-B" were obtained from the Xe^{136}/Xe^{132} ratios on the assumption that Pesyanoe xenon is a mixture of solar-type Xe and trapped chondritic Xe. The Xe^{136}/Xe^{132} ratio of the 1000° fraction is used here as the best available choice for solar-type xenon. It is interesting, however, to speculate that the δ-values of solar-type Xe^{134} and Xe^{136} could be slightly more negative. If they matched

Table 2. Relative abundances of the rare gases.

Source	He^4/Ne^{20}	Ne^{20}/Ar^{36}	Ar^{36}/Kr^{84}	Kr^{84}/Xe^{132}
Pesyanoe-A	388	16.4	2,270	7.5
Pesyanoe-B	388	16.4	2,500	13.0
Atmosphere	0.318	0.522	48.5	27.8
Average, chondrites			~200	1.3
Cosmic abundance:				
Aller (*12*)	355	72	6,760	30
Suess and Urey (*13*)	400	61	4,300	27
Cameron (*14*)	1000	13	18,000	13

the solid line shown in Fig. 1, this would be an indication that terrestrial atmospheric and solar-type xenon may be related to each other by a strong mass fractionating process (*11*). Trapped chondritic xenon, on the other hand, may possibly be related to solar-type xenon by the superposition on the latter of fission-xenon components with the required relative mass yields.

KURT MARTI
Chemistry Department, University of California at San Diego, La Jolla

References and Notes

1. K. Marti, paper presented at the 31st annual meeting of the Meteoritical Society, Cambridge, Massachusetts, 1968.
2. N. Grögler and K. Marti, in preparation.
3. K. Marti, *Earth Planet. Sci. Lett.* **3**, 243 (1967); O. Eugster, P. Eberhardt, J. Geiss, *ibid.*, p. 249.
4. A. O. Nier, *Phys. Rev.* **79**, 450 (1950).
5. K. Marti, P. Eberhardt, J. Geiss, *Z. Naturforsch.* **21a**, 398 (1966); M. W. Rowe, D. D. Bogard, P. K. Kuroda, *J. Geophys. Res.* **71**, 4679 (1966); C. M. Hohenberg, M. N. Munk, J. H. Reynolds, *ibid.* **72**, 3139 (1967).
6. P. Eberhardt, O. Eugster, J. Geiss, *J. Geophys. Res.* **70**, 4427 (1965).
7. M. N. Munk, *Earth Planet. Sci. Lett.* **3**, 457 (1968); O. Eugster, P. Eberhardt, J. Geiss, *J. Geophys. Res.* **74**, 3874 (1969).
8. O. K. Manuel, *Geochim. Cosmochim. Acta* **31**, 2413 (1967).
9. P. Signer and H. E. Suess, in *Earth Science and Meteoritics*, J. Geiss and E. E. Goldberg, Eds. (North-Holland, Amsterdam, 1963).
10. J. Zähringer, *Z. Naturforsch.* **17a**, 460 (1962).
11. D. Krummenacher, C. M. Merrihue, R. O. Pepin, J. H. Reynolds, *Geochim. Cosmochim. Acta* **26**, 231 (1962).
12. L. H. Aller, *The Abundance of the Elements* (Interscience, New York, 1961).
13. H. E. Suess and H. C. Urey, *Rev. Mod. Phys.* **28**, 53 (1956).
14. A. G. W. Cameron, in *Handbook of Geophysics and Space Environments* (U.S. Air Force Cambridge Research Laboratories, Washington, D.C., 1965).
15. I thank E. L. Krinov and G. G. Goles for providing meteorite samples and N. Grögler and J. Geiss for collaboration and discussions. Supported by AEC contract AT(11-1)-34 and NASA contract NAS 9-8107.

15 September 1969

Late Cenozoic Underthrusting of the Continental Margin off Northernmost California

Abstract. *The presence of magnetic anomaly 3, age 5 million years, beneath the continental slope off northernmost California, is evidence for underthrusting of the continental margin during the late Cenozoic. Folded and faulted strata near the base of the slope attest to deformation of the eastern edge of the turbidite sediments in the Gorda Basin; the deformation observed is exactly that expected from underthrusting. The relative motions of three crustal plates also suggest underthrusting, possibly with a major component of right-lateral slip.*

Sea-floor spreading (*1*) and plate tectonics (*2, 3*) have provided a working model of global tectonic activity. A major problem, with important implications for continental geology, is the nature of deformation of continental margins that form the boundary between two crustal plates (*4*). The continental margin off northernmost California (Fig. 1) is such a boundary, and the structure of the margin, the magnetic anomalies of the sea floor, and the interpreted relative motions of crustal plates all suggest late Cenozoic underthrusting of the margin.

The structure of the continental margin was studied by reflection profiling, magnetic profiling, and bottom sampling. A series of north- to northwest-trending anticlines crops out on the continental slope (*5*) and dams turbidites that form the surface of a marginal plateau (Fig. 2). The folds are cut by faults with dip separations predominantly west side down. The anticlinal ridges yield fossiliferous fine-grained dolomite and limestone. The foraminifera in the rocks represent a maximum age of Miocene (*6*), but none of the species present are extinct.

Magnetic anomalies, associated with the Mason-Raff anomaly pattern of the northeastern Pacific (*7*), are mapped over the continental slope off the California-Oregon border (Fig. 1). The easternmost positive anomaly is correlated with anomaly number 3 (*8*). The estimated age of 5 million years for this anomaly (*1*) is probably very close because Cox and others (*9*) have dated the reversals radiometrically back to 4.5 million years. The presence of anomaly 3 beneath the continental slope suggests differential movement of the oceanic crust beneath the continental margin.

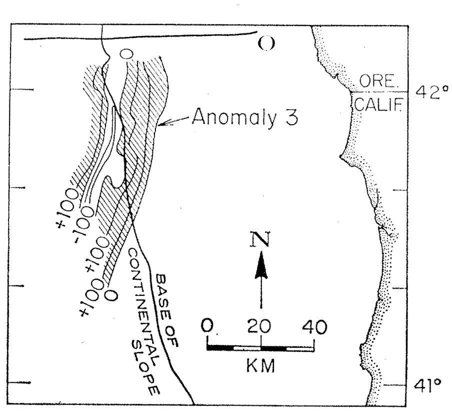

Fig. 1. Magnetic anomalies mapped on the continental slope off northernmost California. Shaded anomalies are positive. Contour interval is 100 gammas. The location of profile *O* is indicated.

West of the slope (Fig. 2) is a thick section of horizontal strata, probably turbidites, filling a structural depression or trench at the base of the slope. Underlying the turbidite section are several hundred meters of poorly reflecting pelagic sediment draping the irregular basement topography. The superposition of turbidites on pelagic material suggests either a sudden change in depositional regime or a continuous process of conveying oceanic crust toward, and thrusting it under, the continental margin. The ridge at 52 km (Fig. 2) consists of folded strata acoustically similar to, and essentially as thick as, the layered basin deposits. This observation suggests deformation and uplift of the eastern edge of the Gorda Basin deposits. Compression of a tabular body of mechanically weak sediments against a continental margin in the process of underthrusting should produce deformation only on the leading or landward edge of the sediment body. The deformation observed at the base of the slope is compatible with underthrusting.

In order to determine the direction and rate of differential motion between the Gorda Basin and the continental margin, the relative velocities of three major crustal plates must be considered—the American, Pacific, and Gorda Plates (Fig. 3). While the Gorda may be considered as a single plate (*2*), account must be taken of the deformation of magnetic anomalies within the Gorda Basin (*1, 7*). Bending of the anomalies indicates more rapid spreading from the northern part of the Gorda Rise than from the southern part. Retardation in the southern part may be caused by impingement of the Gorda-Mendocino Escarpment on the southern edge of the Gorda Plate.

The relative velocity of the Gorda Plate with respect to the continental margin (G_a) is found by adding the motion of the Pacific Plate relative to North America (P_a) to that of the Gorda Plate relative to the Pacific (G_p) (Fig. 3). Both deformation within the Gorda Plate (*10*) and possible overthrusting of the Pacific Plate along the